Supporting Information

Cai *et al.* 10.1073/pnas.0810232105

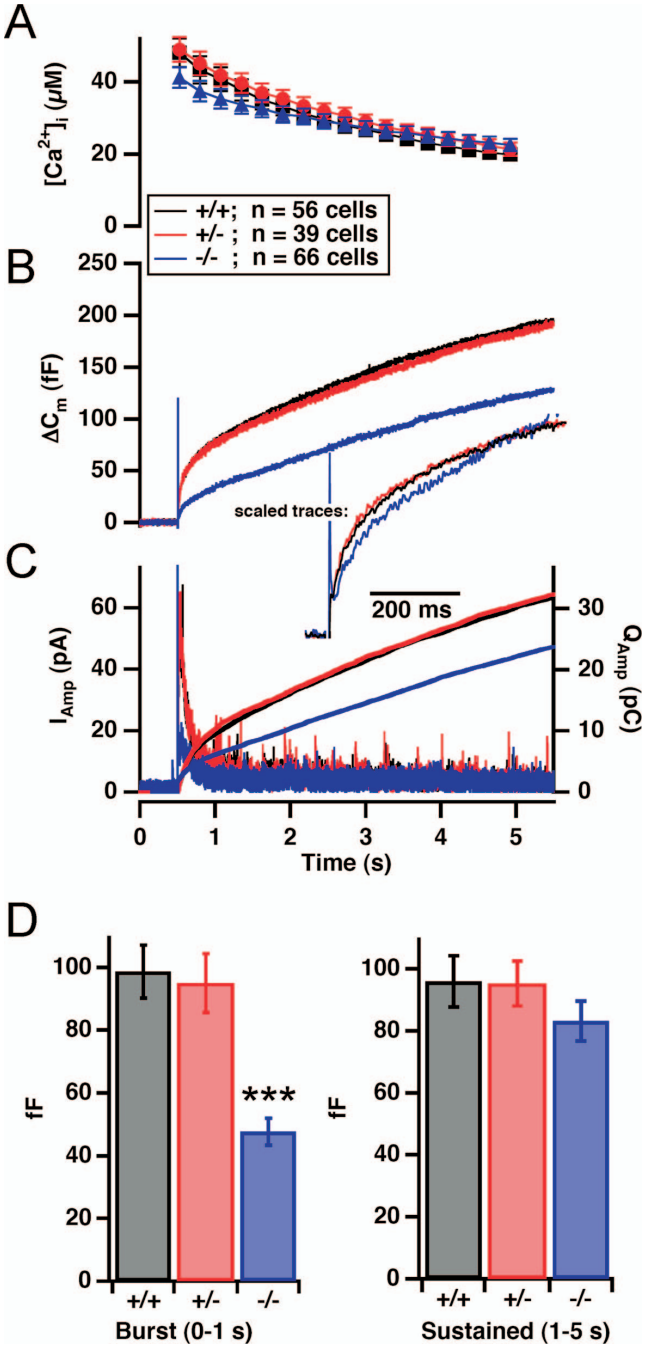

Fig. S1. Exocytosis triggered by photolyzing caged Ca^{2+} at ≈500 nM basal calcium concentration. (*A–C*) Averaged intracellular Ca^{2+} concentration (*A*), averaged secretion as monitored with membrane capacitance measurements (*B*) and with amperometry (*C*) from CPX $II^{-/-}$ (blue), heterozygous (red) and WT (black) cells. (*Inset*) C_m traces were scaled to the same amplitude at 1 sec after flash to compare the kinetics of C_m increases. The amperometric traces were also integrated to show the cumulative secretion (*C*). (*D*) Analysis of the size of burst phase (0–1 sec after flash) and sustained phase (1–5 sec after flash) by capacitance measurements. Number of cells is indicated in *A*. The burst size in CPX $II^{-/-}$ cells was significantly (***, $P < 0.001$, one-way ANOVA with Tukey–Kramer posttest) smaller than both CPX $II^{+/-}$ and CPX $II^{+/+}$ cells.

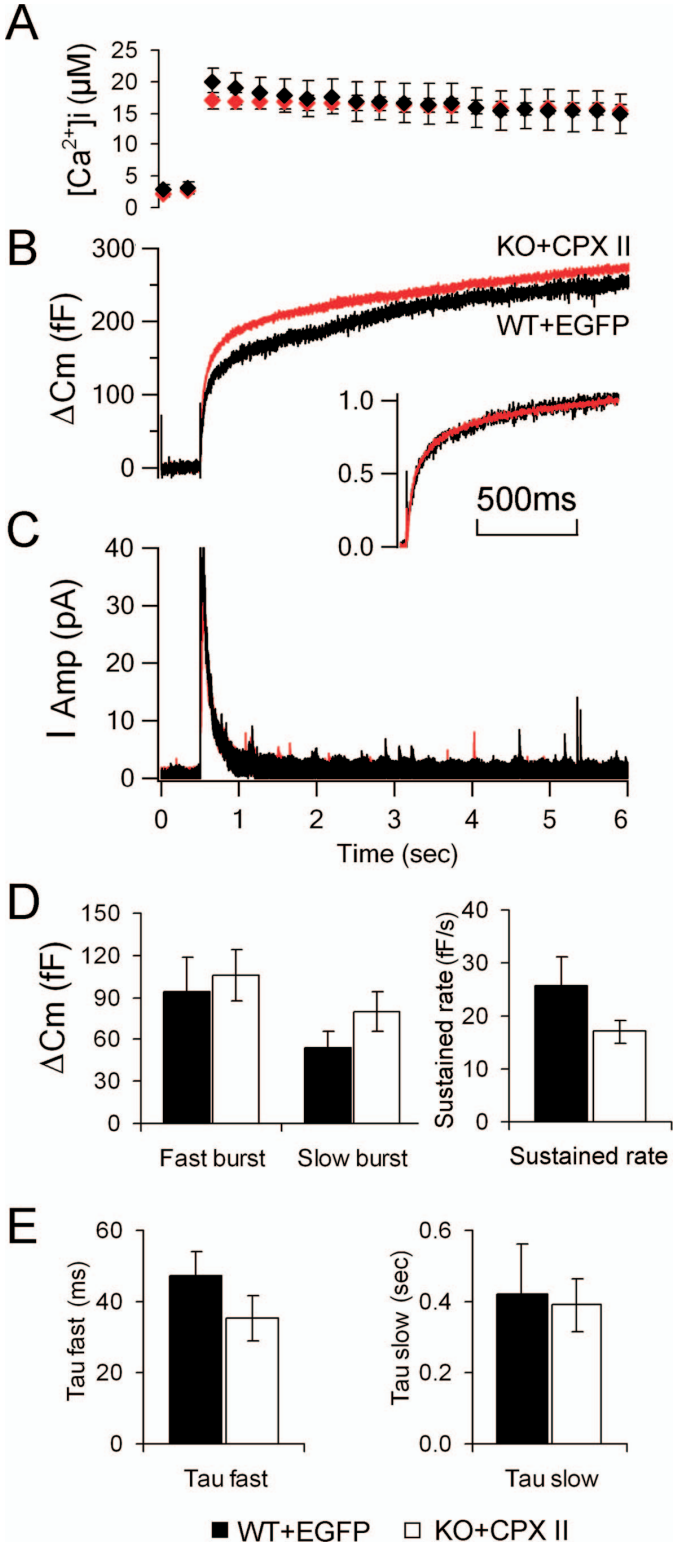

Fig. S2. Rescued secretion triggered by photolyzing caged Ca^{2+}. (*A–C*) Averaged intracellular Ca^{2+} concentration (*A*), averaged secretion as monitored with membrane capacitance measurements (*B*) and with amperometry (*C*) from WT cells expressing only EGFP (black) and CPX II$^{-/-}$ cells rescued with CPX II (red). (*Inset*) C_m traces were scaled to the same amplitude at 1 s after flash to compare the kinetics of C_m increases. (*D*) Analysis of the size of burst phases and sustained rate of secretion by capacitance measurements. Data were averaged from 8 experiments from 6 WT cells express EGFP, 3 animals (black, $n = 8$); 18 experiments from 12 CPX II$^{-/-}$ cells rescued with CPX II, 4 animals (white, $n = 18$). (*E*) Analysis of the time constants of the fast and slow bursts of secretion (WT, black, $n = 5$; CPX II KO, white, $n = 18$). Data were shown as mean ± SEM.

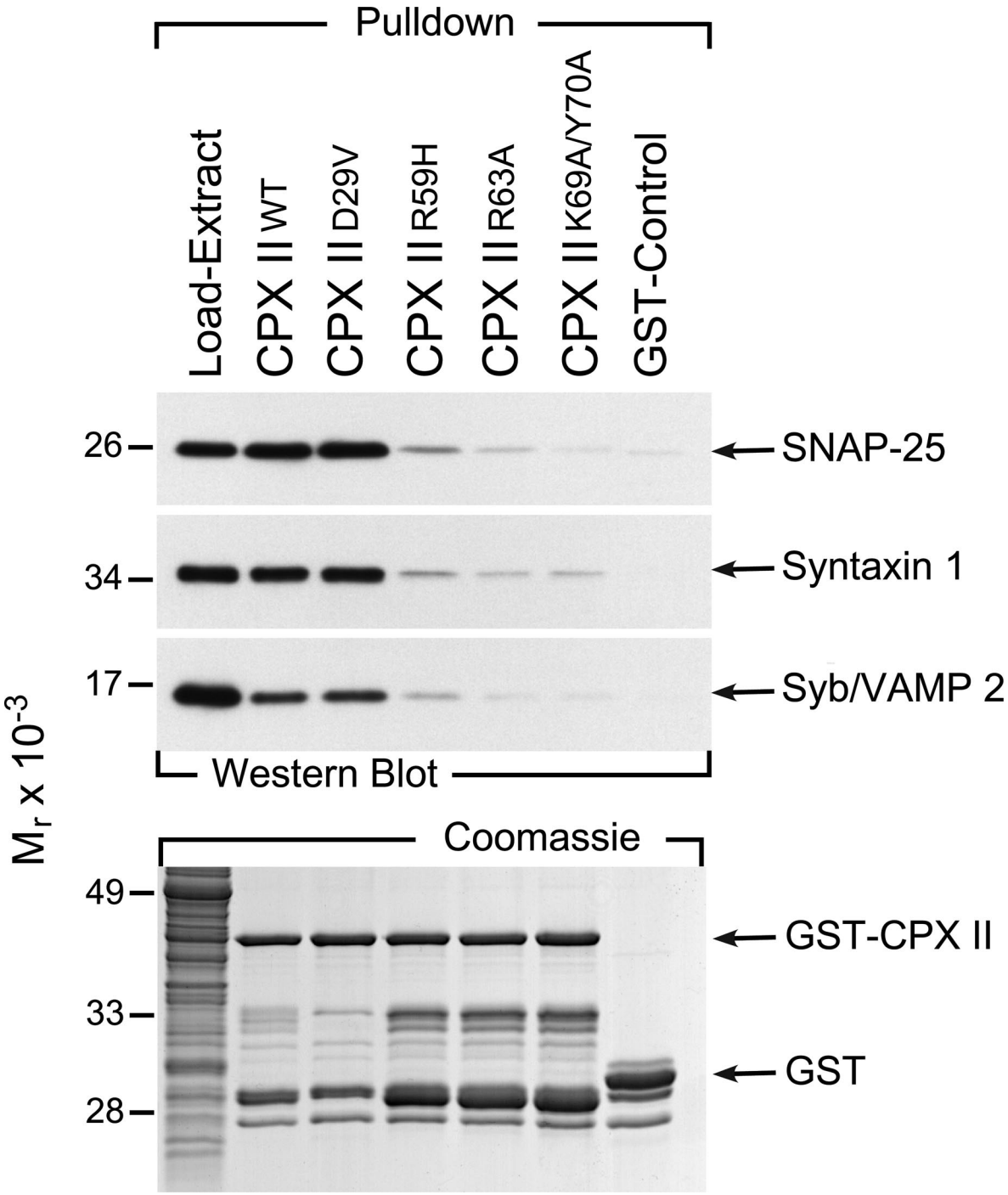

Fig. S3. Representative cosedimentation assay of WT GST-CPX II, mutant GST-CPX II (D29V, R59H, R63A, K69A/Y70A) fusion proteins and GST alone. GST-CPX II WT and the mutant GST-CPX II D29V show normal SNARE complex binding, while mutants GST-CPX II R59H, GST-CPX II R63A and GST-CPX II K69A/Y70A show reduced binding to the SNARE complex.

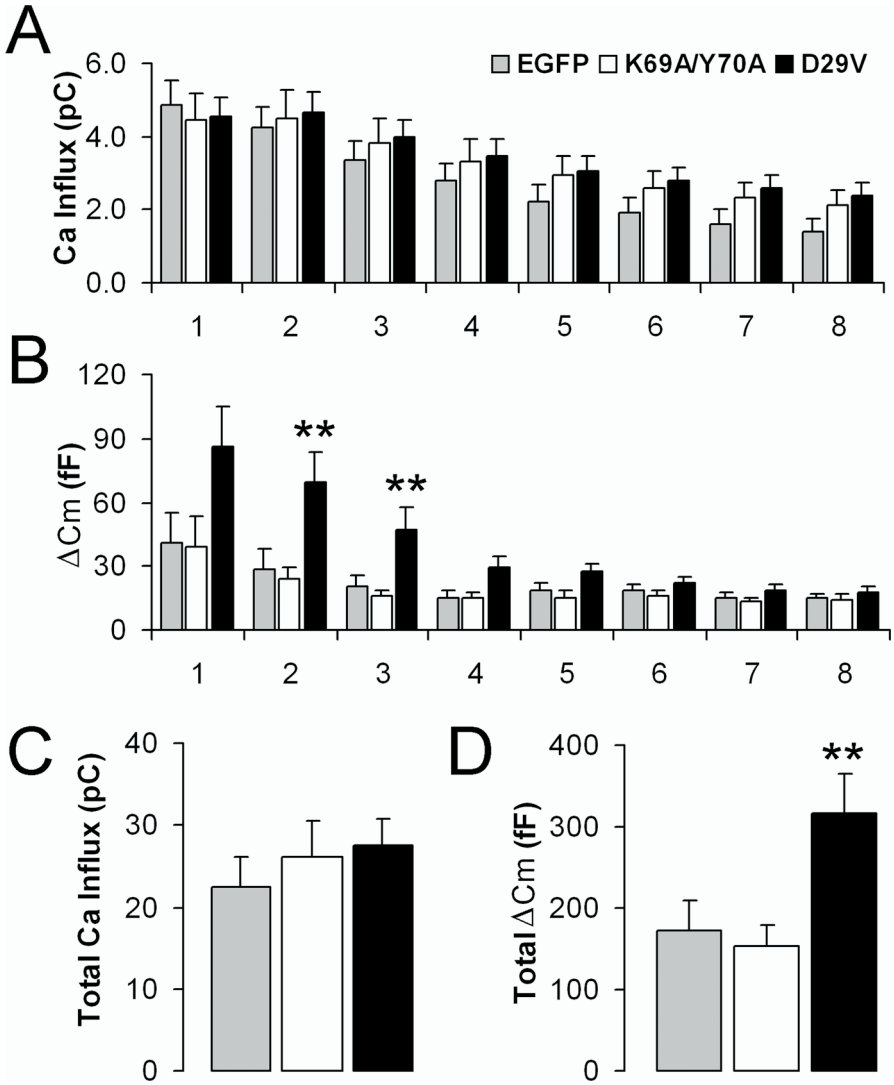

Fig. S4. Exocytosis in CPX II$^{-/-}$ cells expressing different CPX mutants. (*A* and *B*) Ca^{2+} influxes and ΔC_m in response to each of the eight 100-ms depolarizations. (*C* and *D*) Total Ca^{2+} influx and total ΔC_m (summed over all eight depolarizations). Based on the cosedimentation results (Fig. S3), we picked CPX II D29V as the mutant with normal SNARE binding and CPX II K69A/Y70A as the mutant with reduced SNARE binding for the experiments. Data were averaged from 18 experiments from 13 CPX II$^{-/-}$ cells expressing EGFP (gray, $n = 18$), 29 experiments from 18 CPX II$^{-/-}$ cells expressing CPX II K69A/Y70A and EGFP (white, $n = 29$), and from 16 experiments from 9 CPX II$^{-/-}$ cells expressing CPX II D29V and EGFP (black, $n = 16$). Data are expressed as mean ± SEM. **, $P < 0.03$.

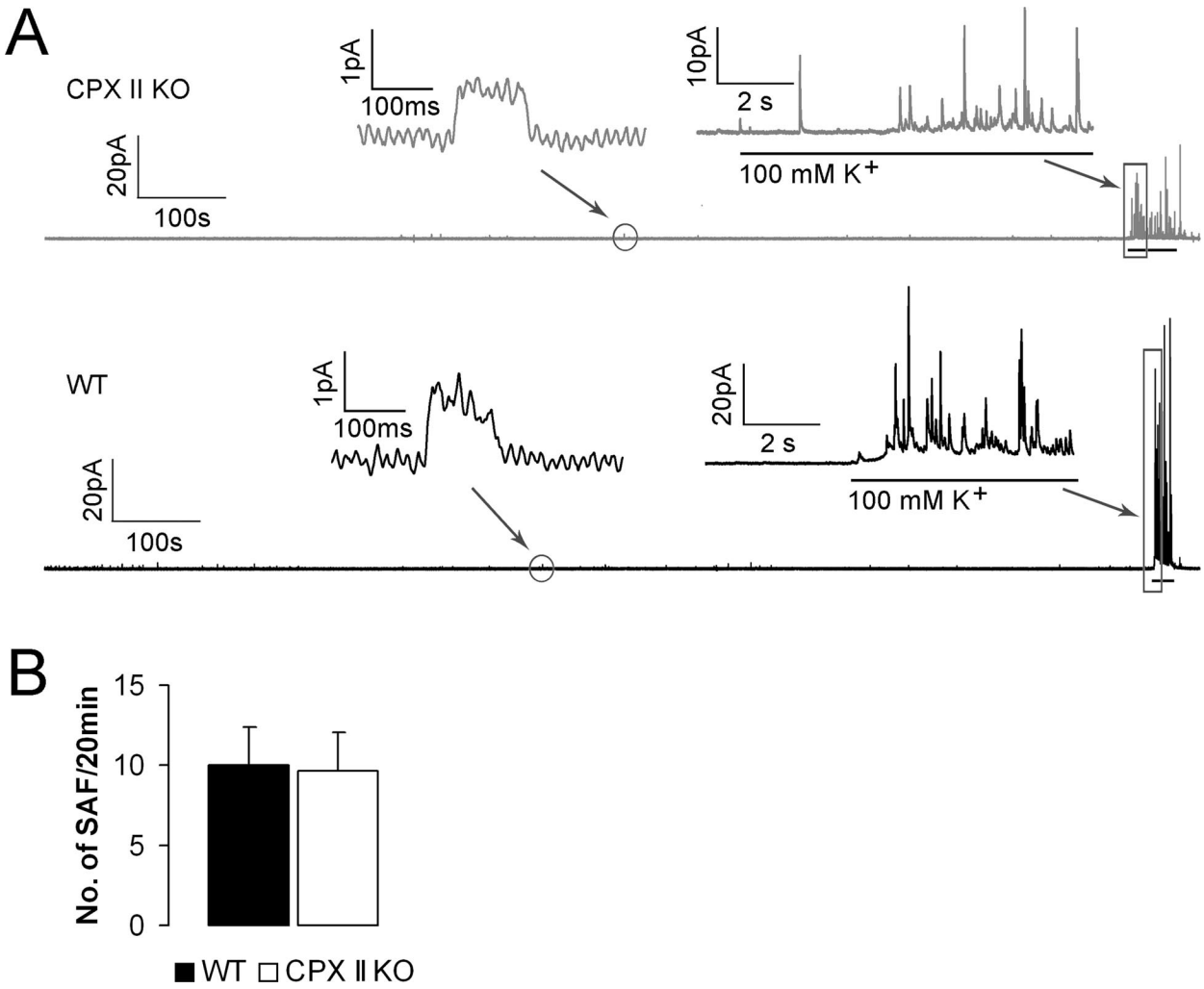

Fig. S5. Spontaneous release in CPX II$^{-/-}$ and WT cells. (*A*) Sample traces of CPX II$^{-/-}$ (*Upper*) and WT (*Lower*) cells. (*Inset*) the stand-alone foot (SAF) (in the circle) and spikes after high K^+ stimulus (in the square frame) are amplified to show detail. Traces were filtered at 100Hz to view SAF. (*B*) Number of SAF during the 20 min recording from CPX II$^{-/-}$ (CPX II KO, white, $n = 9$ cells) and WT (WT, black, $n = 7$ cells) cells.